Hindawi Publishing Corporation
International Journal of Photoenergy
Volume 2013, Article ID 650973, 6 pages
http://dx.doi.org/10.1155/2013/650973

Research Article

Effects of Titanium Oxide Nanotube Arrays with Different Lengths on the Characteristics of Dye-Sensitized Solar Cells

Chin-Guo Kuo,[1] Cheng-Fu Yang,[2] Lih-Ren Hwang,[3] and Jia-Sheng Huang[1]

[1] *Department of Industrial Education, National Taiwan Normal University, Taipei, Taiwan*
[2] *Department of Chemical and Materials Engineering, National University of Kaohsiung, Kaohsiung 811, Taiwan*
[3] *Department of Automation and Control Engineering, Chung Chou University of Science and Technology, Changhua County, Taiwan*

Correspondence should be addressed to Cheng-Fu Yang; cfyang@nuk.edu.tw

Received 2 January 2013; Revised 15 February 2013; Accepted 18 February 2013

Academic Editor: Sih-Li Chen

The self-aligned highly ordered TiO_2 nanotube (TNT) arrays were fabricated by potentiostatic anodization of Ti foil, and we found that the TNT-array length and diameter were dependent on the electrolyte (NH_4F) concentration in ethylene glycol and anodization time. The characteristics of the fabricated TNT arrays were characterized by XRD pattern, FESEM, and absorption spectrum. As the electrolyte NH_4F concentration in the presence of H_2O (2 vol%) with anodization was changed from 0.25 to 0.75 wt% and the anodization period was increased from 1 to 5 h, the TNT-array length was changed from 9.55 to 30.2 μm and the TNT-array diameter also increased. As NH_4F concentration was 0.5 wt%, the prepared TNT arrays were also used to fabricate the dye-sensitized solar cells (DSSCs). We would show that the measured photovoltaic performance of the DSSCs was dependent on the TNT-array length.

1. Introduction

Since the phenomenon of photocatalytic splitting of water on nanostructure TiO_2 electrodes was discovered in 1972 [1], extensive investigations have been devoted to improve the photocatalytic efficiency of TiO_2-based photo electrodes. TiO_2 is a wide bandgap (anatase 3.2 eV and rutile 3.0 eV) n-type semiconductor, and TiO_2-based photo electrodes have been studied in many fields, such as photocatalysis, dye-sensitized solar cells (DSSCs), and gas sensors because of its outstanding physical, chemical, and optical properties [2–4]. A great advantage of the nanoparticle (NP)-DSSCs is that TiO_2 nanoparticles have a large surface area for dye adsorption, but diffusion, limited by traps, for electron transport in NP-DSSCs impedes the efficiency of conversion of light to electricity [5, 6]. To improve the efficiency of charge collection by promoting both more rapid electron transport and slower charge recombination, several methods with TiO_2 films constructed of oriented one-dimensional (1D) nanostructures have been established. Compared with nanoparticles, TiO_2 nanowires and nanotubes have 1D nanostructures and are suggested to be superior in chemical and photo electrochemical performance, due to its one-dimensional channel for carrier transportation, in which the recombination of e^-/h^+ is expected to be reduced. For that, DSSCs based on one-dimensional TiO_2 nanowires have been reported. One-dimensional TiO_2 such as nanotube is more attractive due to its large specific surface area and well-defined charge carriers transport path. Because the surface area of TiO_2 nanotube (TNT) arrays is higher than that of TiO_2 nanowires due to the additional surface area enclosed inside the hollow structure.

Anodic oxidation is a powerful and efficient technique for fabricating highly ordered TNT arrays [7, 8]. The highly ordered TNT arrays exhibited good performance when used as a photo electrode, due to the unique nanostructure that facilitates separation of the photoexcited charges and results in higher charge collection efficiencies [9]. Of a variety of TiO_2 synthesis strategies, particular interest has been given to the anodic oxidized growth of TNT layers on Ti foil, as it leads to an array of closely packed vertically aligned tubes [7, 10, 11]. A self-assembled TNT arrays can be fabricated by anodic oxidation of Ti foil in HF-containing acidic electrolyte. In contrast to random nanoparticle systems where slow electron

diffusion typically limits device performance [12, 13], the precisely oriented nature of the crystalline (after annealing) TNT arrays makes them excellent electron percolation pathways for vectorial charge transfer between interfaces [13]. In this study, the TNT arrays with different lengths were fabricated on the Ti substrates by varying the anodization period and changing the aqueous electrolytes to organic electrolytes. 20 nm Pt on transparent conductive ITO glass was used as the electrode to increase the conductivity. In the past, only few researches were used to discuss the effects of TNT arrays with different lengths on the characteristics of DSSCs. We would investigate the TNT arrays in the applications of the DSSCs, and we would also investigate the effects of the TNT-array length on the properties of the investigated DSSCs.

2. Experimental

We fabricated ordered nanochannel TNT arrays at 25°C on anodizing titanium (Ti) foil (Aldrich, 99.7% purity) as square discs (50 mm × 50 mm) at a constant voltage of 60 V. The electrolyte solutions contained ammonium fluoride (NH_4F, 99.9%; 0.25, 0.5, and 0.75 wt%) in EG in the presence of H_2O (2 vol%, pH = 6.8) with anodization for varied periods (1–5 h). Ti foils, 0.25 mm thick, were degreased by ultrasonication in acetone and then isopropanol, respectively, for about 30 min, followed by rinse with deionized (DI) water, and finally dried in the air before being used. Highly ordered TNT arrays over large areas were prepared by a potentiostatic anodization in a two-electrode electrochemical cell with a platinum (Pt) sheet as counter electrode. All anodization experiments were carried out at room temperature. The Ti foils were anodized in a concentration of 0.25 wt%, 0.50 wt%, and 0.75 wt% NH_4F (98+% ACS reagent) and ethylene glycol (99.8% anhydrous) solution. For the two-step process, the TNT arrays were first rinsed with ethanol, dried in air, and annealed at 150°C for 2 h to remove organic solvents. Then they were then crystallized at 450°C for another 1 h in an air furnace. The structure of the fabricated DSSCs was shown in Figure 1, which was different from the most reported structures; the effective area in this study was 40 mm × 40 mm, and 20 nm Pt was deposited on ITO by using sputter method to increase the conductivity. As Figure 1 shows, the preparation of the DSSCs on the TNT/Ti foils was composed of four steps: (i) fabrication of TNT arrays on Ti foils by anodization, (ii) annealing the TNT array/Ti foil, (iii) deposition Pt onto ITO glass, and (iv) formation of the DSSCs.

The TiO_2 electrodes were immersed into the N-719 (Solaronix, Aubonne, Switzerland) dye solution (0.5 mM in ethanol) and were held at room temperature for 24 h to adsorb the dye molecules. The dye-treated TiO_2 electrodes were rinsed with ethanol and dried under nitrogen flow. The amount of N-719 dye absorbed on the TNT arrays was measured with a UV-visible-NIR spectrophotometer equipped with an integrating sphere. The liquid electrolyte was prepared by dissolving 0.1 M of lithium iodide (LiI), 0.01 M of iodine (I_2), 0.6 M of 1-butyl-3-methylimidazolium iodide (BMII), 0.1 M of guanidinium thiocyanate (GuNCS), and 0.5 M of 4-tert-butylpyridine (TBP) in acetonitrile/valeronitrile (85 : 15 v/v). Current-voltage characteristic of the fabricated DSSCs was measured using a Keithley 2400 source meter under simulated AM 1.5G illumination (100 mW cm^{-2}) provided by a solar simulator (69920, 1 kW Xe lamp with an optical filter, Oriel) to determine the open-circuit voltage (V_{oc}), short-circuit current (J_{sc}), fill factor (FF), and conversion efficiency (η). Photocurrent densities were measured in a standard three-electrode configuration with the TNT arrays as a photo-anode electrode, Pt-ITO foil as the counter electrode, and a saturated calomel electrode (SCE) as the reference electrode.

Figure 1: Structure of the fabricated DSSCs.

3. Results and Discussion

X-ray diffraction (XRD) patterns were used to characterize the structure of the anodized TNT arrays. As shown in Figure 2, the mainly crystalline phase of the as-prepared TNT arrays was amorphous. As compared with the JCPDS files, the diffraction peaks of Ti and rutile TiO_2 phases could be found, and these diffraction peaks were not enhanced as the TNT-array length increased. It is noted that the anatase TiO_2 peaks are much worse than the Ti and rutile TiO_2 peaks, so it is reasonable to neglect the influences of such trace anatase TiO_2 content in the as-prepared TNT arrays. As TNT arrays were annealed at 450°C for 1 h, the diffraction peaks of anatase TiO_2 were clearly observed. For the free-standing TNT arrays, the diffraction peaks of Ti substrate disappeared, and the rutile TiO_2 phase was still observed, most of the diffraction peaks could be attributed to the anatase TiO_2 phase. The diffraction peaks at about 2θ = 25.5°, 37.3°, 38.1°, 48.2°, 54.2°, and 55.2° are indexed to the (101), (103), (004), (200), (105), and (211) crystal faces of anatase TiO_2 phase (PDF card 75-1537, JCPDS).

Figure 3 shows the variations in the TNT-array length, the samples are prepared in different NH_4F concentrations (0.25 wt%, 0.50 wt%, and 0.75 wt%) and ethylene glycol solution at an anodization potential of 60 V for different time (1 h, 3 h, and 5 h), respectively. For a 0.25 wt% NH_4F concentration and anodization at, respectively, a time of 1 h, 3 h, and 5 h, an increase in TNT-array length from about 9.55 μm, 15.7 μm to 19.8 μm was observed. Also, as the NH_4F concentration increased from 0.50 wt% to 0.75 wt%, an increase in the TNT-array length with increasing anodization time was also observed. As the same anodization time was used, higher NH_4F concentration resulted in TNT arrays with larger diameters and longer lengths (will be shown in Figure 4). We attribute the increase in TNT-array length with larger

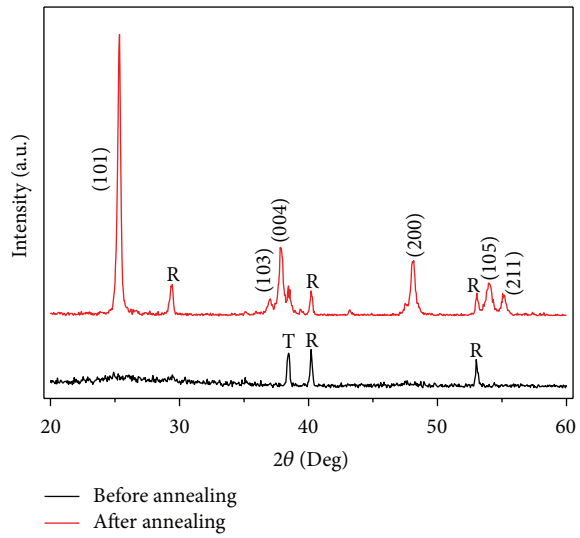

FIGURE 2: Comparison on the XRD patterns of TNT arrays before and after annealing.

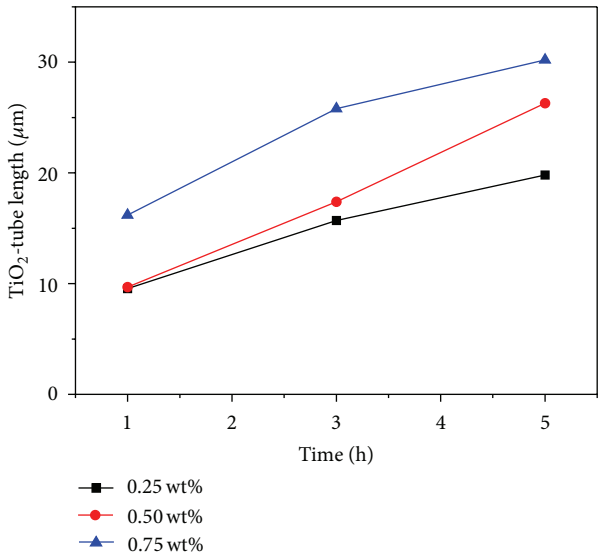

FIGURE 3: TNT-array length as a function of NH_4F concentration and anodization time.

NH_4F concentration to the increased reaction chances for ionic transport through the barrier layer at the bottom of the pore, and that can result in faster movement of the Ti/TiO_2 interface into the Ti metal.

Figure 4 shows the SEM top- and cross-section views of TNT arrays anodized at 60 V for a 0.50 wt% NH_4F concentration and anodization at, respectively, a time of 1 h, 3 h, and 5 h. It is evident that the highly ordered TNT arrays consist of very regular tubes with different inner diameters, which are dependent on the anodization time. Figures 4(a), 4(c), and 4(e) show that these TNT arrays have overall similar lengths and have very smooth walls typical of nanotubes grown in Ti substrates. The as-anodized TNT arrays are typically amorphous (as Figure 2 shows), and they can be crystallized by annealing in air. The evolution of the surface morphology as a result of annealing shows that the regular tubular structure remains stable until around 450°C. The whole TNT arrays remained intact being stood on the Ti substrates, even for the TNT arrays with a length as short as 9.68 μm (Figure 4(b)) and as long as 26.3 μm (Figure 4(f)). Figures 4(b), 4(d), and 4(f) clearly display the cross-section of the two-step anodized TNT films, where a structure of bilayers can be seen: the top layer of crystallized TNT arrays and the bottom layer of titanium substrate. There is no significant change in the pore diameter or wall thickness even after annealing at 450°C for 1 h. However, when the annealing temperature is increased to 550°C, the tubular structure of the fabricated TNT arrays completely collapses leaving many deep and large cracks (not shown here).

Figure 5 shows the UV-vis diffusion reflectance spectra of the annealed TNT arrays dipped in N-719 for 24 h, for a 0.50 wt% NH_4F concentration and anodization at a time of 1 h, 3 h, and 5 h, respectively. In the UV and visible light regions, the absorption intensity of the TNT arrays increased with the increase of the TNT-array length. Therefore, we can assume a better photoelectrochemical capability under UV light as the longer TNT arrays are used as an electrode. The sharp band gap absorption edges of the three kinds of TiO_2 nanotube arrays were all around 385 nm. In the meantime, a small shift of the threshold toward the visible light region (red shift phenomenon) was observed for the 5 h samples. For the shorter sample, on the other hand, the onset was closer to the ultraviolet region (blue shift phenomenon). The band gap energy of pure TiO_2 estimated with the Kubelka-Munk function is about 3.34 eV [14]. It is clear that even with the different lengths the annealed TNT arrays as well as the mixture of the antase and rutile crystalline phases might not make the band gap energy change. Figure 5 also shows an important result that in the visible light region, the absorption intensity increased with increasing TNT-array length, which revealed that the TNT arrays with longer length were more sensitive to visible light than those of the short ones. Therefore, we can assume a better photoelectrochemical capability of the longer TNT-array electrode under visible light. Consequently, the UV-vis spectra suggest that the longer TNT arrays might exhibit the higher solar light response than the shorter ones, and the increase in the photovoltaic performance with the increase of the TNT-array length is expectable.

The current-voltage characteristics of the DSSCs (substrate size 40 × 40 mm^2) under illumination are measured, and the photo current density versus voltage curves of the TNT-based DSSCs is shown in Figure 6, for the TNT arrays growing at a 0.50 wt% NH_4F concentration and anodization at a time of 1 h, 3 h, and 5 h, respectively. For comparison, the TNT arrays with the lengths of 9.68 μm, 17.4 μm, and 26.3 μm on Ti substrates with back-side irradiation were investigated. Table 1 lists the values of open-circuit voltage (V_{oc}), short-circuit current density (J_{sc}), fill factor (F.F.), and efficiency (η) for the developed DSSC devices. The filter factor is defined as the ratio of the maximum power from the solar cell to the product of V_{oc} and I_{sc} and shown as

$$\mathrm{FF} = \frac{I_m V_m}{I_{sc} V_{oc}}, \tag{1}$$

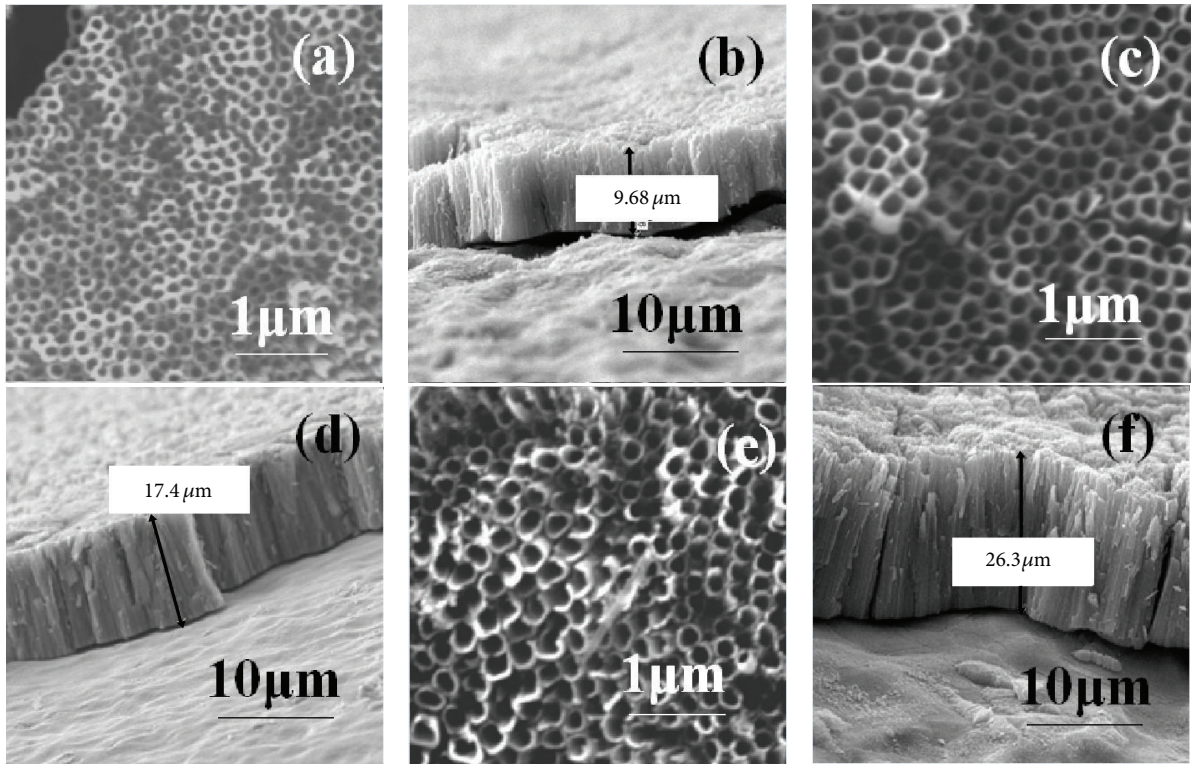

Figure 4: SEM images of 0.5 wt% $NH_4F + 2H_2O$ + EG TNT arrays after cleaning, anodization, and annealing for varied periods. Top views for (a) 1 h, (c) 3 h, and (e) 5 h and side views for (b) 1 h, (d) 3 h, and (f) 5 h, respectively.

Table 1: Values of open-circuit voltage (V_{oc}), short-circuit current density (J_{sc}), fill factor (FF), and efficiency (η) for solar cells with different length of the TiO_2 nanotube.

Length (μm)	V_{oc} (mV)	J_{sc} (mA/cm^2)	FF	η (%)	η (%, 30 days)
9.68	652	8.87	0.50	2.93	2.75
17.4	681	10.16	0.49	3.46	3.28
26.3	712	11.32	0.49	4.09	3.92

where V_{oc} is the open-circuit voltage, I_{sc} is the short-circuit current density, I_m and V_m are the current and voltage at the maximum output.

With an increase of the TNT-array length from 9.68 μm to 26.3 μm, J_{sc} increased from 8.87 mA cm^{-2} to 11.30 mA cm^{-2} and the V_{oc} increased from 652 mV to 709 mV. TNT arrays have a one-dimensional channel for carrier transportation that promotes electron transport. An important implication of the longer transport pathway is that electrons undergo more trapping and detrapping events, which imply that the longer TNT arrays may increase the efficiency. This can be possibly attributed to the increase in the number of adsorbed dye molecules from the increased surface area of the TNT arrays and, therefore, a higher number of photogenerated electrons. However, when the TNT-array length increased from 9.68 μm to 26.3 μm, an unnotable decrease in η value was found. The efficiency of the solar cells increased from 2.89% (TNT-array length = 9.68 μm) to 3.46% (TNT-array length = 17.4 μm) with increased TNT-array length. Moreover, the efficiency could be raised to 4.09% when the TNT-array length was increased to 26.3 μm. The greater efficiency is mainly ascribable to the increased short-circuit current density. Obviously, the light harvesting efficiency of dye molecules adsorbed on the TNT-based photo anode would reach saturation for the TNT arrays at a given length, which would be around 25 μm [15]. However, because as 20 nm Pt is deposited on the ITO, the Pt/ITO bilayer electrode will decrease the transmittance ratio of light; we believe that this is the reason to cause the decrease in the efficiency of the fabricated DSSCs. The reliability problem of dye-sensitized solar cell is always an important issue, and it is that broken electrochemical system by leaking electrolyte that makes solar cell lose its photovoltaic generating capacity. In general, reliability evaluation criteria can be categorized in the following four ways: dry heat cycle test, heat-humidity cycle test, light soaking test, and heat-humidity test. Table 1 also shows that after using light soaking test (after certain optical irradiation under 1 sun condition and then performance test.) for 30 days the fill factors decrease from 2.03 to 2.75, from 3.46 to 3.28, and from 4.09 to 3.92 as the TNT-array lengths are 9.68 μm, 17.4 μm, and 26.3 μm, respectively,. Recently, Jennings et al. had reported that the peak of IPCE

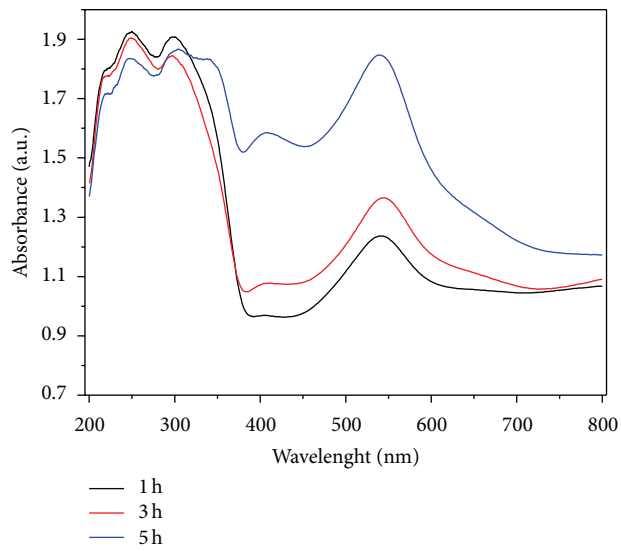

Figure 5: Absorption spectra of TNT arrays sensitized with N-719 dye at various TNT-array lengths produced with 0.5 wt% NH_4F concentration, under simulated AM-1.5 solar illumination (100 mW cm^{-2}) and active area 0.28 cm^2.

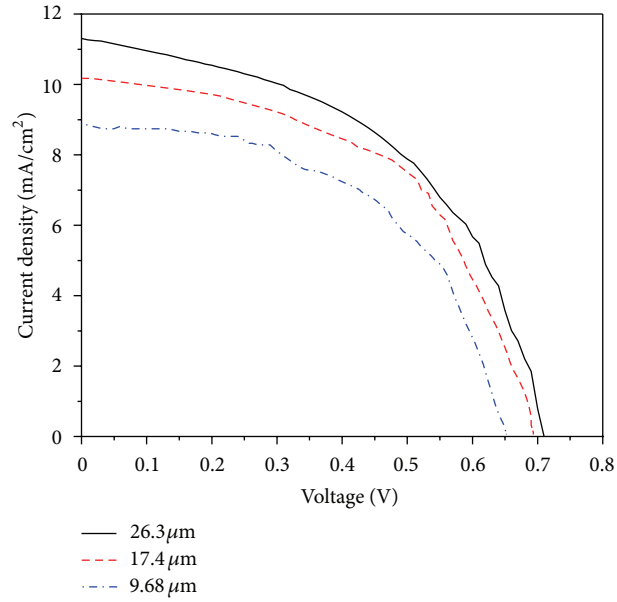

Figure 6: Current-voltage characteristics of the dye-sensitized solar cells under illumination.

reached 90% and the collection efficiency for the photo-injected electrons was close to 100% for a 20 μm TNT array [15]. In this study, the TNT-array lengths are all below or around the optimal length, and an enhancement of J_{sc} and V_{oc} with an increase in TNT-array length may be attributed to the increase in the number of absorbed dye molecules. Beyond that, increasing the TNT-array length could not further enhance light harvesting.

4. Conclusion

In this study, TNT arrays with different lengths were successfully fabricated. After annealing at 450°C for 1 h, the diffraction peaks of anatase TiO_2 phase were clearly observed in the prepared TNT arrays. The TNT-array length increased with the increases of NH_4F concentration and anodization time. A shift of the absorption threshold toward the visible light region was observed for the 5 h sample, and the band gap absorption edges of the developed TNT arrays were all around 385 nm. With an increase of TNT-array length from 9.68 μm to 26.3 μm in the DSSC devices, the J_{sc} increased from 8.87 mA cm^{-2} to 11.30 mA cm^{-2}, the V_{oc} increased from 652 mV to 709 mV, and the photovoltaic performance increased from 3.12% to 4.09%. After using light soaking test for 30 days the fill factors decreased from 2.03 to 2.75, from 3.46 to 3.28, and from 4.09 to 3.92 as the TNT-array lengths were 9.68 μm, 17.4 μm, and 26.3 μm, respectively.

Acknowledgment

The authors acknowledge financial supports from NSC 101-2514-S-003-004-, NSC 101-3113-S-262-001-, and 99-2221-E-390-013-MY2.

References

[1] A. Fujishima and K. Honda, "Electrochemical photolysis of water at a semiconductor electrode," *Nature*, vol. 238, no. 5358, pp. 37–38, 1972.

[2] Y. Chiba, A. Islam, R. Komiya, N. Koide, and L. Han, "Conversion efficiency of 10.8% by a dye-sensitized solar cell using a TiO_2 electrode with high haze," *Applied Physics Letters*, vol. 88, no. 22, Article ID 223505, 2006.

[3] N. Kopidakis, N. R. Neale, K. Zhu, J. Van De Lagemaat, and A. J. Frank, "Spatial location of transport-limiting traps in TiO_2 nanoparticle films in dye-sensitized solar cells," *Applied Physics Letters*, vol. 87, no. 20, Article ID 202106, pp. 1–3, 2005.

[4] C. G. Wu, C. C. Chao, and F. T. Kuo, "Enhancement of the photo catalytic performance of TiO_2 catalysts via transition metal modification," *Catalysis Today*, vol. 97, no. 2-3, pp. 103–112, 2004.

[5] N. Lu, X. Quan, J. Li, S. Chen, H. Yu, and G. Chen, "Fabrication of boron-doped TiO_2 nanotube array electrode and investigation of its photoelectrochemical capability," *Journal of Physical Chemistry C*, vol. 111, no. 32, pp. 11836–11842, 2007.

[6] B. X. Lei, J. Y. Liao, R. Zhang, J. Wang, C. Y. Su, and D. B. Kuang, "Ordered crystalline TiO_2 nanotube arrays on transparent FTO glass for efficient dye-sensitized solar cells," *Journal of Physical Chemistry C*, vol. 114, no. 35, pp. 15228–15233, 2010.

[7] M. Paulose, K. Shankar, S. Yoriya et al., "Anodic growth of highly ordered TiO_2 nanotube arrays to 134 μm in length," *Journal of Physical Chemistry B*, vol. 110, no. 33, pp. 16179–16184, 2006.

[8] J. M. Macak, H. Tsuchiya, L. Taveira, S. Aldabergerova, and P. Schmuki, "Smooth anodic TiO_2 nanotubes," *Angewandte Chemie*, vol. 44, no. 45, pp. 7463–7465, 2005.

[9] K. Zhu, N. R. Neale, A. Miedaner, and A. J. Frank, "Enhanced charge-collection efficiencies and light scattering in dye-sensitized solar cells using oriented TiO_2 nanotubes arrays," *Nano Letters*, vol. 7, no. 1, pp. 69–74, 2007.

[10] D. Gong, C. A. Grimes, O. K. Varghese et al., "Titanium oxide nanotube arrays prepared by anodic oxidation," *Journal of Materials Research*, vol. 16, no. 12, pp. 3331–3334, 2001.

[11] Q. Chen and D. Xu, "Large-scale, noncurling, and free-standing crystallized TiO_2 nanotube arrays for dye-sensitized solar cells," *Journal of Physical Chemistry C*, vol. 113, no. 15, pp. 6310–6314, 2009.

[12] G. K. Mor, K. Shankar, M. Paulose, O. K. Varghese, and C. A. Grimes, "Use of highly-ordered TiO_2 nanotube arrays in dye-sensitized solar cells," *Nano Letters*, vol. 6, no. 2, pp. 215–218, 2006.

[13] A. J. Frank, N. Kopidakis, and J. V. D. Lagemaat, "Electrons in nanostructured TiO_2 solar cells: transport, recombination and photovoltaic properties," *Coordination Chemistry Reviews*, vol. 248, no. 13-14, pp. 1165–1179, 2004.

[14] T. C. An, X. H. Zhu, and Y. Xiong, "Feasibility study of photoelectrochemical degradation of methylene blue with three-dimensional electrode-photocatalytic reactor," *Chemosphere*, vol. 46, no. 6, pp. 897–903, 2002.

[15] J. R. Jennings, A. Ghicov, L. M. Peter, P. Schmuki, and A. B. Walker, "Dye-sensitized solar cells based on oriented TiO_2 nanotube arrays: transport, trapping, and transfer of electrons," *Journal of the American Chemical Society*, vol. 130, no. 40, pp. 13364–13372, 2008.